

# Formation and properties of some antimony-doped strontium titanate ceramics

A. IANCULESCU, A. BRĂILEANU<sup>a\*</sup>, G. VOICU, N. DRĂGAN<sup>a</sup>, D. CRIȘAN<sup>a</sup>

University "Politehnica" Bucharest, 1-7 Gh. Polizu, 011061 Bucharest, Romania

<sup>a</sup>Institute of Physical Chemistry "I. G. Murgulescu" of Romanian Academy, 202 Spl. Independenței, 060021 Bucharest, Romania

Ceramics of  $\text{SrTi}_{1-x}\text{Sb}_x\text{O}_3$  ( $0 \leq x \leq 0.015$ ) composition were prepared by solid state reaction. Samples were obtained after sintering in air at 1300 and 1400 °C, respectively, with a soaking time of 3 hours. Even at 1000 °C, XRD data point out, single phase compositions for all samples studied. Above a critical Sb proportion ( $x = 0.0075$ ) the microstructure changes and an abnormal grain growth process starts to occur. Besides, the dielectric losses start to decrease and the interfacial polarization increases, leading to the increase of the overall effective permittivity, up to a maximum value of  $\sim 4500$  for  $x = 0.01$ . The microstructure feature mentioned, as well as the dielectric behaviour are correlated with the change of the supplementary charge compensation induced by  $\text{Sb}^{5+}$  donor dopant, from an electronic mechanism toward an ionic (by Sr vacancies) one.

(Received January 18, 2006; accepted March 23, 2006)

**Keywords:** Defects, Grain size, Microstructure, Dielectric properties,  $\text{SrTiO}_3$

## 1. Introduction

$\text{SrTiO}_3$  is one of the widely used materials in the electronic ceramic industry as semiconductor material at high temperatures or as dielectric material for internal boundary layer capacitors (IBLC), due to its high dielectric constant and excellent stability with temperature and applied voltage [1-3].

Donor-type dopants are often added in order to improve the electrical properties of  $\text{SrTiO}_3$ -based ceramics both through changes in defect structure of the perovskite lattice as well as in microstructure of the obtained ceramics [4-10].

In the present study, the formation and the characteristics of undoped and Sb-doped strontium titanate ceramics were studied as a function of Sb dopant concentration.

## 2. Experimental

### 2.1. Samples preparation

Ceramic samples of  $\text{SrTi}_{1-x}\text{Sb}_x\text{O}_3$  ( $x = 0; 0.0025; 0.005; 0.0075; 0.01$  and  $0.015$ ) composition were prepared by classical ceramic method from p.a. grade oxides and carbonates:  $\text{TiO}_2$  (Merck),  $\text{Sb}_2\text{O}_3$  (Merck) and  $\text{SrCO}_3$  (Fluka), by a wet homogenization technique in isopropanol.

The initial mixtures were dried and shaped by uniaxial pressing at 160 MPa into pellets of 20 mm diameter and  $\sim 3$  mm thickness. The pellets were thermally treated in air in the temperature range of 1000-1400 °C with 3h plateau.

The samples pre-sintered at 1100 °C were grounded, pressed again using an organic binder (PVA) and then sintered in air for 3 hours, at 1300 and 1400 °C, respectively.

### 2.2. Samples characterization

Phase composition evolution in isothermal conditions was investigated by X-ray diffraction, by means of a Shimadzu XRD 600 diffractometer.

The microstructure of the samples was examined by scanning electron microscopy, using a Hitachi S2600N equipment.

The sinterability of the samples was evaluated by linear shrinkage, apparent density and porosity measurements.

To estimate the electric behaviour of the sintered materials, electrical measurements of capacitance and dielectric losses were performed at room temperature and at 500 Hz frequency, using a Hewlett Packard 4284 A LCR-meter.

## 3. Results and discussion

XRD data obtained for all six mixtures isothermally treated for 3 hours in the temperature range of 1000 – 1200 °C and slowly cooled at room temperature point out the presence of the characteristic diffraction maxima of the single phase  $\text{SrTiO}_3$  compound or  $\text{SrTi}_{1-x}\text{Sb}_x\text{O}_3$  solid solutions, which has the ideal perovskite structure (Fig. 1).

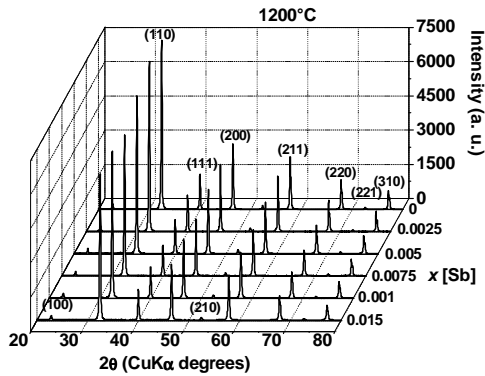
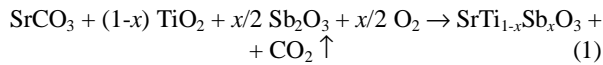


Fig. 1. X-ray diffraction patterns of the  $SrTi_{1-x}Sb_xO_3$  solid solutions, isothermally treated at 1200 °C/3h.

The increase of Sb content determines no phase composition changes, proving that the isomorphy limit of antimony in  $SrTiO_3$  lattice was not reached yet. These results are in agreement with those reported by Burn *et al* [11]. Antimony incorporated as  $Sb^{3+}$  ( $Sb_2O_3$ ), oxidizes to  $Sb^{5+}$  during the thermal treatment and replaces  $Ti^{4+}$  in the perovskite lattice, due to the small difference between ionic radii of the substitute ( $r_{Ti^{4+}} = 0.68 \text{ \AA}$ ) and of the substituent ( $r_{Sb^{5+}} = 0.62 \text{ \AA}$ ) in the studied concentration range, so that  $SrTi_{1-x}Sb_xO_3$  solid solutions are formed, according to the reaction (1):



With the temperature rise, for all six samples a more pronounced crystallinity reflected in the increase of the characteristic diffraction peaks intensities of the solid solutions was observed. The evolution of the (110) diffraction peak intensity with the temperature and antimony content is presented in Fig. 2. At 1000 and 1100 °C the intensity of the (110) diffraction peak is almost constant with the antimony concentration. The influence of the dopant is more obvious at 1200 °C, where a slight decreasing tendency of the same diffraction maximum can be observed because of the disturbance of the crystalline ordering induced by the incorporation of the aliovalent solute.

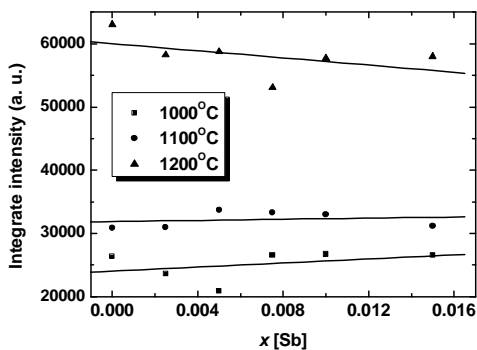
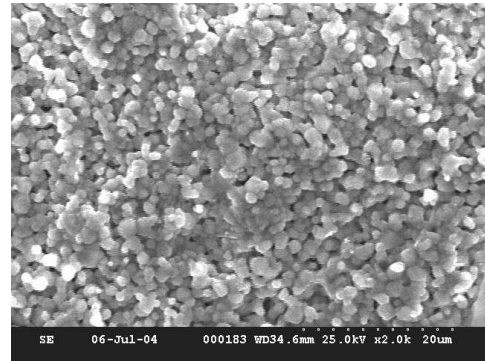
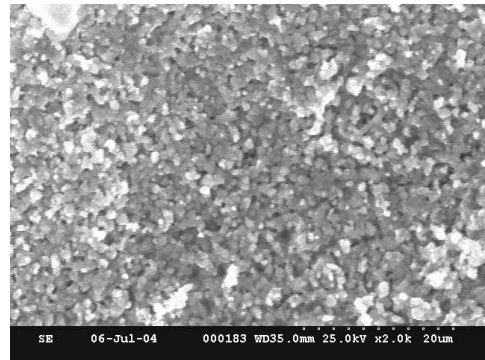


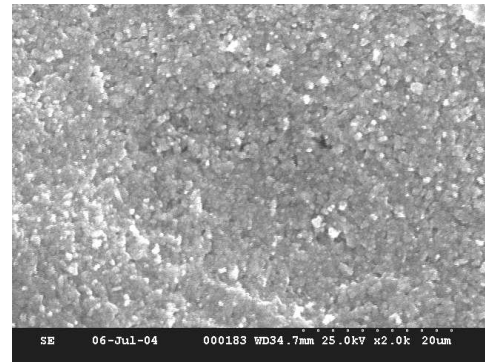
Fig. 2. Evolution of the (110) diffraction peak intensity with the temperature and antimony content.



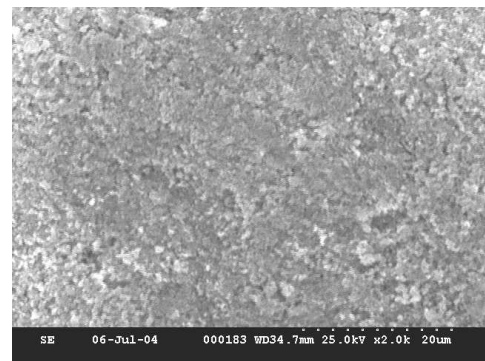
(a)



(b)



(c)



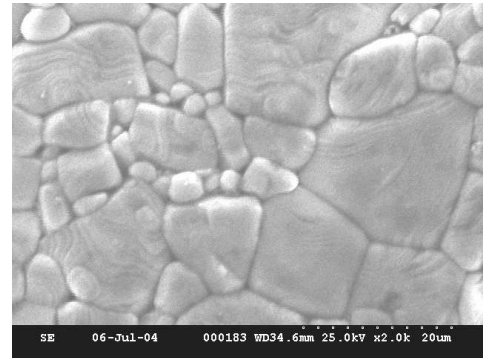
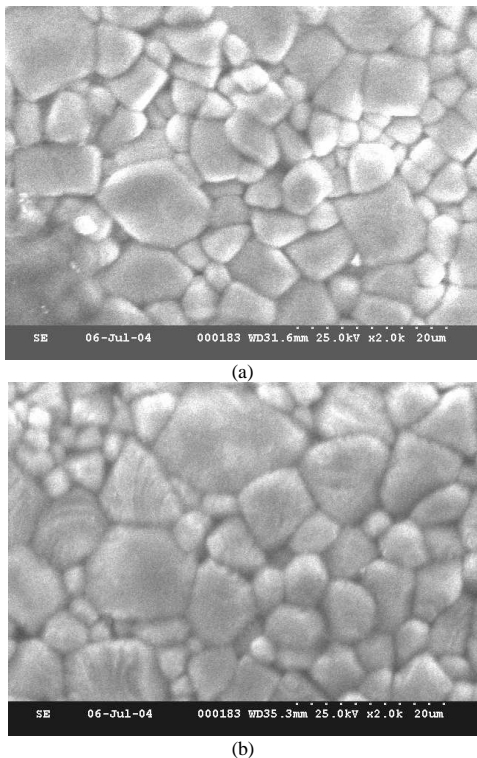
(d)

Fig. 3. SEM micrographs of the compositions sintered at 1300 °C: a)  $SrTiO_3$ ; b)  $SrTi_{0.995}Sb_{0.005}O_3$ ; c)  $SrTi_{0.9925}Sb_{0.0075}O_3$  and d)  $SrTi_{0.985}Sb_{0.015}O_3$ .

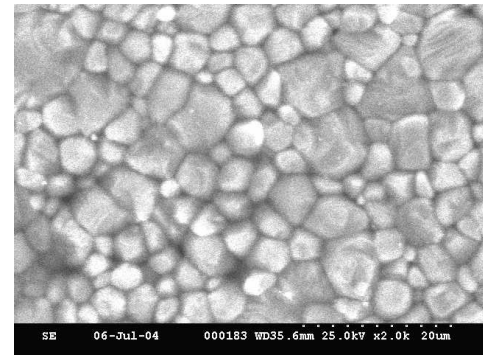
The microstructure of the pure  $\text{SrTiO}_3$  thermally treated at  $1300^\circ\text{C}/3\text{ h}$  is homogeneous, consisting of small, spherical grains of  $\sim 1.6\ \mu\text{m}$  and intergranular pores (Fig. 3(a)). At this temperature, the antimony dopant acts as an inhibitor of the grain growth process, leading to a decrease of the average grain size up to  $0.27\ \mu\text{m}$  for the sample with the highest antimony content ( $x = 0.015$ ) (Fig. 3(b)-(d)).

SEM analyses, performed on samples sintered at  $1400^\circ\text{C}$  reveal for pure  $\text{SrTiO}_3$  a dense microstructure, consisting of larger, homogeneously distributed grains with the main size of  $10\ \mu\text{m}$  (Fig. 4a).

The small Sb proportion in  $\text{SbTi}_{0.995}\text{Sb}_{0.005}\text{O}_3$  composition (Fig. 4b) does not determine essential changes of the microstructure. The increase of Sb concentration up to the critical value of  $x = 0.0075$  determines an abnormal increase of the grains. Thus, for the solid solution  $\text{SrTi}_{0.9925}\text{Sb}_{0.0075}\text{O}_3$  (Fig. 4c), a non-homogeneous microstructure, consisting both of small grains with  $\phi = 5\ \mu\text{m}$  and very large grains with  $\phi = 20\ \mu\text{m}$  can be observed, although the material is very well densified, with a minimum intergranular porosity. For the ceramic with the highest Sb proportion,  $\text{SrTi}_{0.985}\text{Sb}_{0.015}\text{O}_3$  (Fig. 4d), another spectacular change of the microstructure can be remarked. The larger grains vanish totally and the microstructure is homogeneous from the average grain size point of view, consisting of grains of  $\sim 5\ \mu\text{m}$ . Besides, it is obvious that the decrease of the average grain size induced by the higher antimony concentration is accompanied by the appearance of the intergranular porosity. These microstructure features were reported also by Cho *et al* [8] for their Nb-doped  $\text{SrTiO}_3$  samples, where the critical dopant concentration was strongly influenced by the Sr/(Ti+Nb) ratio.



(c)



(d)

Fig. 4. SEM micrographs of the compositions sintered at  $1400^\circ\text{C}$ : a)  $\text{SrTiO}_3$ ; b)  $\text{SrTi}_{0.995}\text{Sb}_{0.005}\text{O}_3$ ; c)  $\text{SrTi}_{0.9925}\text{Sb}_{0.0075}\text{O}_3$  and d)  $\text{SrTi}_{0.985}\text{Sb}_{0.015}\text{O}_3$

Fig. 5 shows the dependence of the average grain size on the antimony content and sintering temperature.

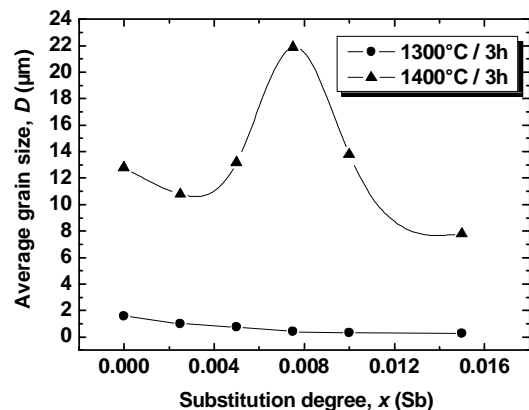
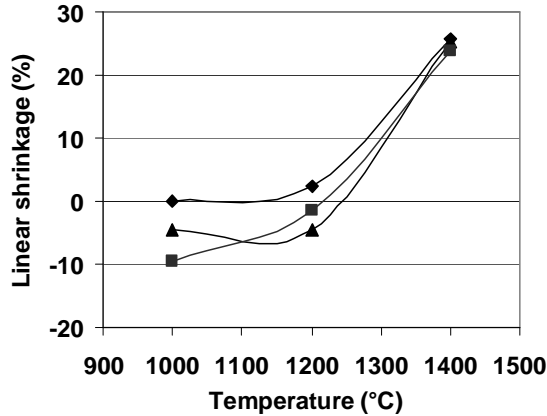


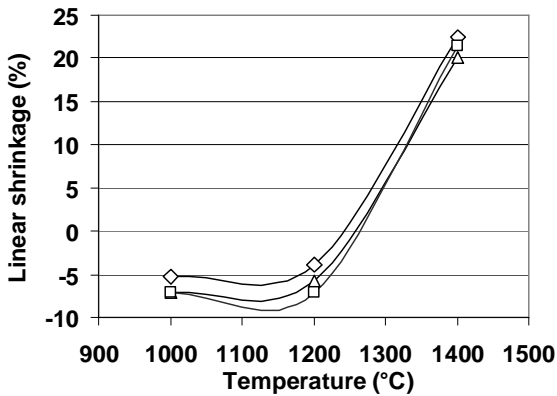
Fig. 5. The average grain size evolution versus the antimony content for samples sintered at  $1300$  and  $1400^\circ\text{C}$ .

The sinterability of the samples was estimated by means of linear shrinkage, apparent density and porosity values. In the first stage of the thermal treatment ( $1000 - 1200^\circ\text{C}$ ) an expansion of all samples irrespective of Sb

content was noticed. Linear shrinkage and therefore samples densification occurs barely in the temperature range of 1200 – 1400 °C (Fig. 6 (a), (b)).



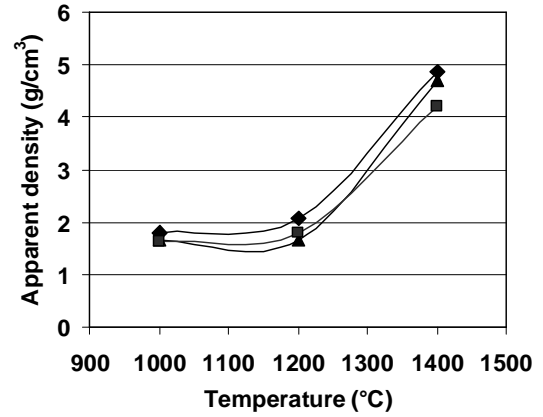
(a)



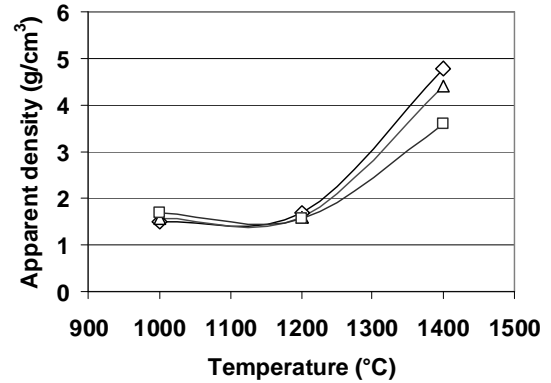
b

Fig. 6. Linear shrinkage as a function of temperature and antimony content ( $x$ ) for calcined samples with: (a)  $\blacklozenge$  -  $x = 0$ ;  $\blacktriangle$  -  $x = 0.0025$ ;  $\blacksquare$  -  $x = 0.005$  and (b)  $\diamond$  -  $x = 0.0075$ ;  $\triangle$  -  $x = 0.01$ ;  $\square$  -  $x = 0.015$ .

These results are sustained also by apparent density and porosity data. Thus the apparent density (Fig. 7 (a), (b)) shows a significant increase in the temperature range mentioned, whereas the apparent porosity decreases drastically from 55 – 70 % at 1300 °C to values ranged between 10 – 30 % at 1400 °C. After the second thermal treatment (sintering), the relative density increases up to ~ 90 – 95% and the apparent porosity decreases to less than 5 % for samples with lower antimony content and to ~ 10 % for highly-doped samples. These results are in good agreement with SEM micrographs.



(a)



(b)

Fig. 7. Apparent density as a function of temperature and antimony content ( $x$ ) for calcined samples with: (a)  $\blacklozenge$  -  $x = 0$ ;  $\blacktriangle$  -  $x = 0.0025$ ;  $\blacksquare$  -  $x = 0.005$  and (b)  $\diamond$  -  $x = 0.0075$ ;  $\triangle$  -  $x = 0.01$ ;  $\square$  -  $x = 0.015$ .

The variations of the relative permittivity and dielectric loss for the samples sintered at 1400 °C as a function of Sb proportion are presented in Fig. 8.

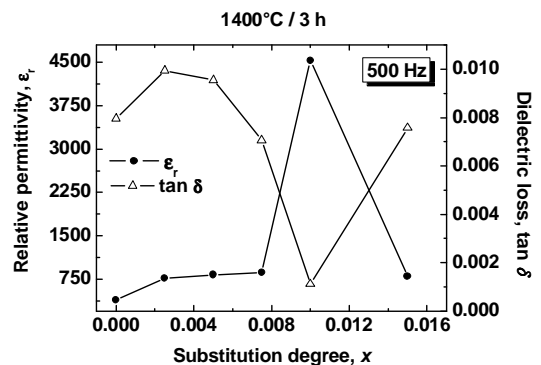
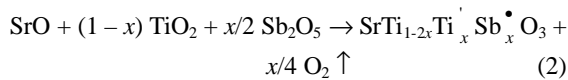
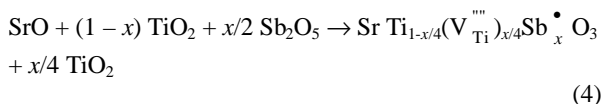
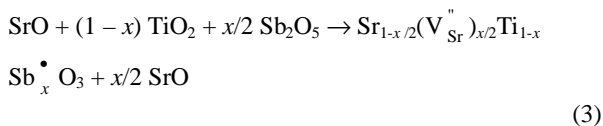


Fig. 8. The evolution of the relative permittivity and dielectric loss against the Sb content at 1400 °C.

For the compositions with  $0 < x \leq 0.0075$ , the increase of the Sb concentration leads to the increase of the charge carrier concentration (electrons) resulted in the partially reduction of  $Ti^{4+}$  to  $Ti^{3+}$ , in order to compensate the supplementary charge induced by the donor dopant, according to the reaction (3):



As a consequence, the maximum value of the dielectric loss is recorded for a Sb proportion of  $x = 0.0025$ . Over the critical value ( $x = 0.0075$ ), the compensation mechanism starts to modify with the increase of the proportion of cation vacancies generated at the grain boundary in order to maintain the electroneutrality of the lattice (eq. (3) and (4)).



Consequently, the dielectric loss decreases (from  $\sim 10^{-2}$  to  $\sim 10^{-3}$ ) and the interfacial polarization increases, leading to an increase of the overall effective permittivity, up to a maximum value of  $\sim 4500$  for  $x = 0.01$ . A similar permittivity evolution against the dopant concentration was found by Chen *et al* [5] for their lanthanum-doped  $SrTiO_3$  solid solutions.

For the Sb proportion  $x > 0.01$ , the cation vacancy concentration increases continuously. These defects tend to distribute uniformly in the whole grain bulk. As a result, the interfacial polarization mechanism starts to be cancelled and the dielectric permittivity decreases. This phenomenon is accompanied by the drastic diminution of the average grain size, as a consequence of the inhibiting effect of the donor dopant on the grain growth process. This involves the porosity increase and therefore higher dielectric losses were recorded. Because of the pronounced decrease of the average grain size, the grain boundary layers, depleted in charge carriers (electrons) and rich in cation vacancies tend to exhibit similar thickness with the grain size. Therefore, homogeneous grains from the point of view of the defect distribution were obtained, which leads to lower relative permittivity values.

Theoretically, both Sr and Ti vacancies could compensate the supplementary charge induced by Sb. The Sr vacancies are much more thermodynamically favourable as compensating defects, in comparison with Ti vacancies in the octahedral interstices. This assumption is sustained by the lack of a Ti-rich secondary phase, which is expected to result according to eq. (4) if the Ti vacancies are the compensating defects. The lack of a Sr-rich secondary phase, according to eq. (3), can be explained in terms of a possible supplementary Sr incorporation into the perovskite structure, by a Ruddlesden-Popper structural accommodation, which involves a superstructure

formation consisting of SrO layers incorporated at  $\sim 30$  perovskite layers [5]. Therefore, in accord with our X-ray diffraction data we concluded that for higher Sb concentrations ( $x > 0.0075$ ), strontium vacancies are the most probable compensating defects in antimony-doped  $SrTiO_3$ .

#### 4. Conclusions

Even at 1000 °C, XRD data point out, for all six compositions studied the presence of the characteristic diffraction maxima of the single phase  $SrTi_{1-x}Sb_xO_3$  solid solution, which has the ideal perovskite structure of  $SrTiO_3$ .

The microstructure of the grains is influenced by the Sb proportion. Pure  $SrTiO_3$  has a dense microstructure which is not much affected by the introduction of small Sb amounts. For higher Sb proportions ( $x = 0.0075$ ) the microstructure changes and an abnormal grain growth process starts to occur. For the ceramics with the highest antimony content a very homogeneous microstructure can be noticed.

This microstructure feature is correlated with the change of compensation mechanism of the supplementary charge induced by the  $Sb^{5+}$  donor dopant. Thus, below a critical antimony concentration ( $x \leq 0.0075$ ) the compensating defects are the electrons resulted in the  $Ti^{4+}$  toward  $Ti^{3+}$  partially reduction, whereas over this concentration value, a strontium vacancy compensation mechanism was assumed as the most probable.

Above this critical Sb concentration the dielectric losses start to decrease and the interfacial polarization increases, leading to the increase of the overall effective permittivity, up to a maximum value of  $\sim 4500$  for  $x = 0.01$ .

#### References

- [1] N. H. Chan, R. K. Sharma, D. M. Smyth, *J. Electrochem. Soc.* **128**, 1762 (1981).
- [2] R. Moos, K. H. Härdtl, *J. Am. Ceram. Soc.* **80**, 2549 (1997).
- [3] R. Waser, *Solid State Ionics* **95**, 89 (1995).
- [4] U. Balachandran, N. G. Eror, *J. Electrochem. Soc.* **129**, 1021 (1982).
- [5] A. Chen, Y. Zhi, *J. Appl. Phys.* **71**, 6025 (1992).
- [6] A. Chen, Y. Zhi, *J. Appl. Phys.* **71**, 4451 (1992).
- [7] T. Inoue, N. Seki, J. -I. Kamimae, K. Eguchi, H. Arai, *Solid State Ionics* **48**, 283 (1991).
- [8] S. G. Cho, P. F. Johnson, *J. Mater. Sci.* **29**, 4866 (1994).
- [9] C. Bae, J. G. Park, Y. H. Kim, H. J. Jeon, *J. Am. Ceram. Soc.* **81**, 3005 (1998).
- [10] A. Ianculescu, A. Brăileanu, M. Zaharescu, S. Guillemet, I. Pasuk, J. Madarász, G. Pokol, *J. Therm. Anal. Cal.* **72**, 173 (2003).
- [11] I. Burn, S. Neirman, *J. Mater. Sci.* **17**, 3510 (1982).

\*Corresponding author: abrail@icf.ro